Supplementary Information

Regulating Surface Oxygen Species on Activated Carbon via Plasma Treatment to Boost Zinc-ion Adsorption for Zinc-ion Hybrid Capacitors

Yongxia Zhang, Xuchao Yang, Xupeng Liu, Yunlong Yang*, Fen Ran*

Energy Storage Institute, State Key Laboratory of Advanced Processing and Recycling of Non-ferrous Metals, School of Material Science and Engineering, Lanzhou University of Technology, School of Green Energy and Energy Storage, Lanzhou 730050, China

Corresponding Authors: Dr. Assistant Prof. Yunlong Yang (ylyang@lut.edu.cn); or Dr. Prof. Fen Ran (ranfen@lut.edu.cn)

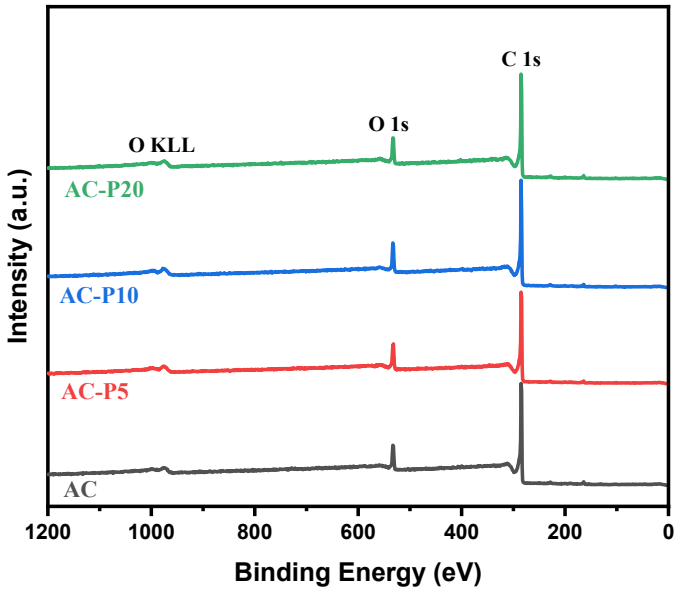

Figure S1. XPS full spectra of AC, AC-P5, AC-P10, and AC-P20.

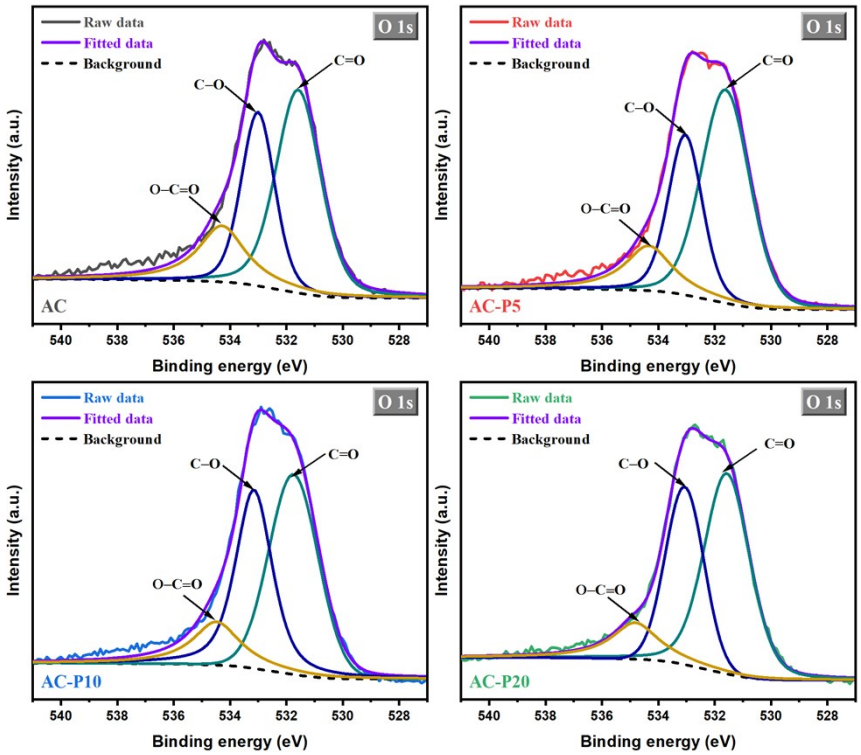

Figure S2. O 1s spectra of AC, AC-P5, AC-P10, and AC-P20.

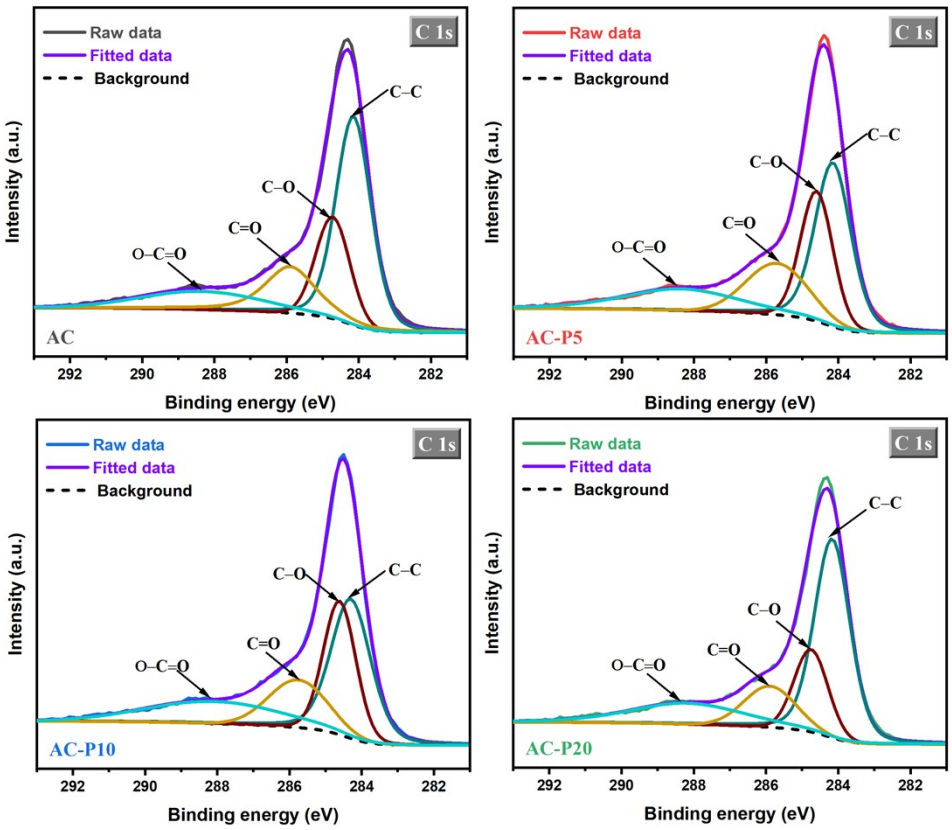

Figure S3. C 1s spectra of AC, AC-P5, AC-P10, and AC-P20.

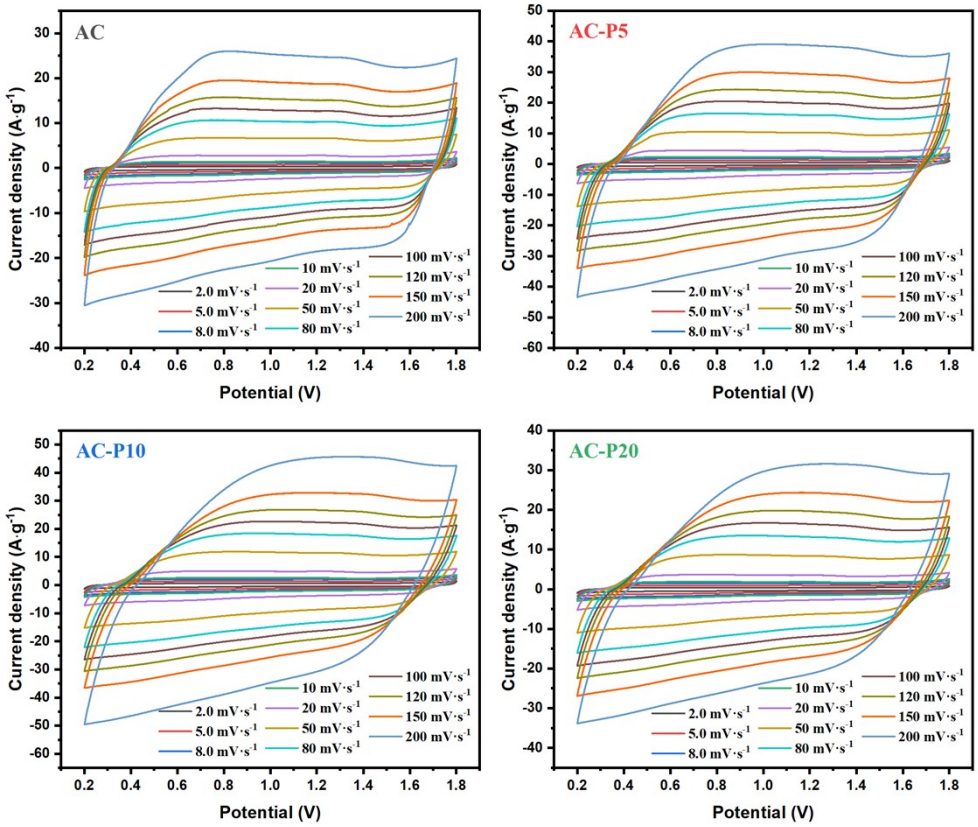

Figure S4. CV curves of AC, AC-P5, AC-P10, and AC-P20 electrodes at different scan rates.

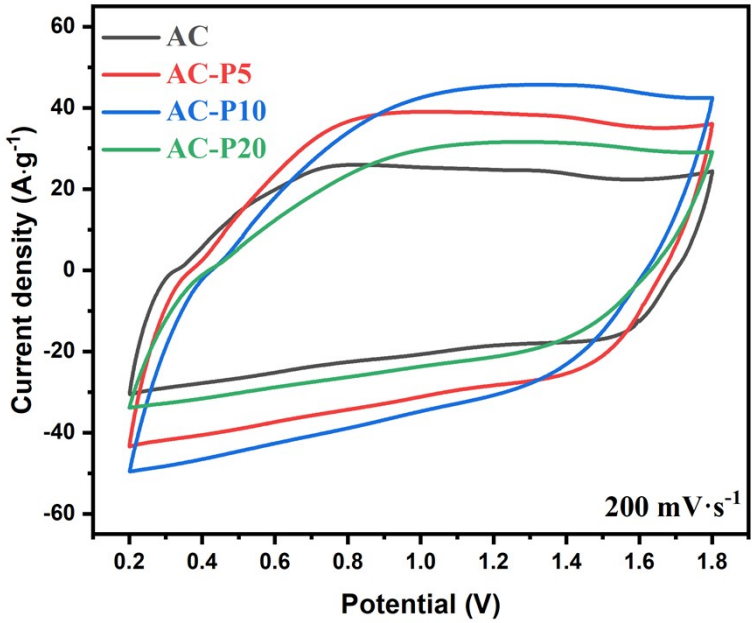

Figure S5. CV curves of AC, AC-P5, AC-P10, and AC-P20 electrodes at 200 mV·s^{-1}.

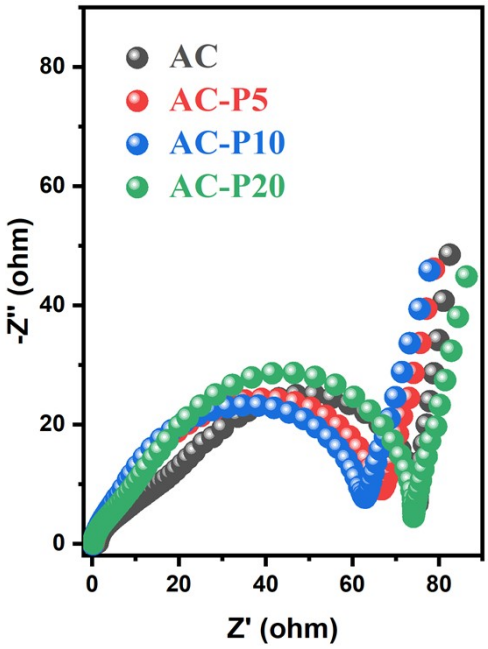

Figure S6. EIS plots of AC, AC-P5, AC-P10, and AC-P20 electrodes, inset shows the equivalent circuit model of all EIS plots.

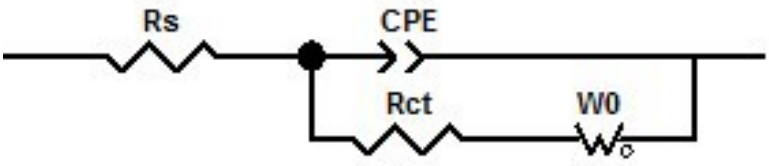

Figure S7. The equivalent electrical circuit model of EIS plots.

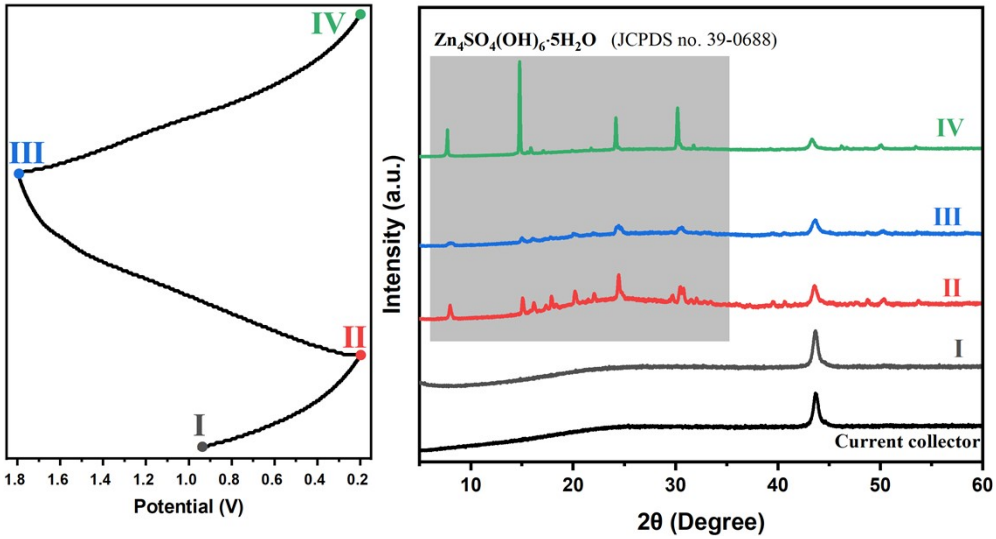

Figure S8. Different states of AC-P10 during charging and discharging, and ex-situ XRD patterns of different states of AC-P10 electrode.

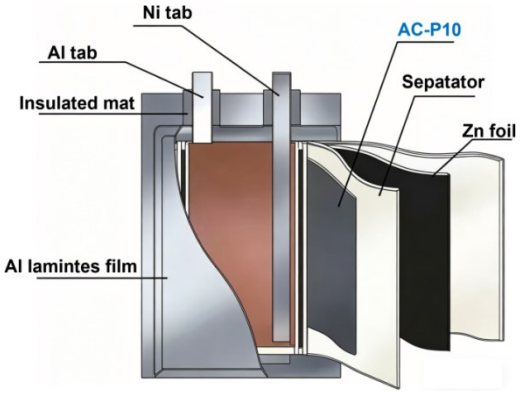

Figure S9. Schematic diagram of the constructed pouch full cell.

Figure S10. Open-circuit voltage of one pouch cell.

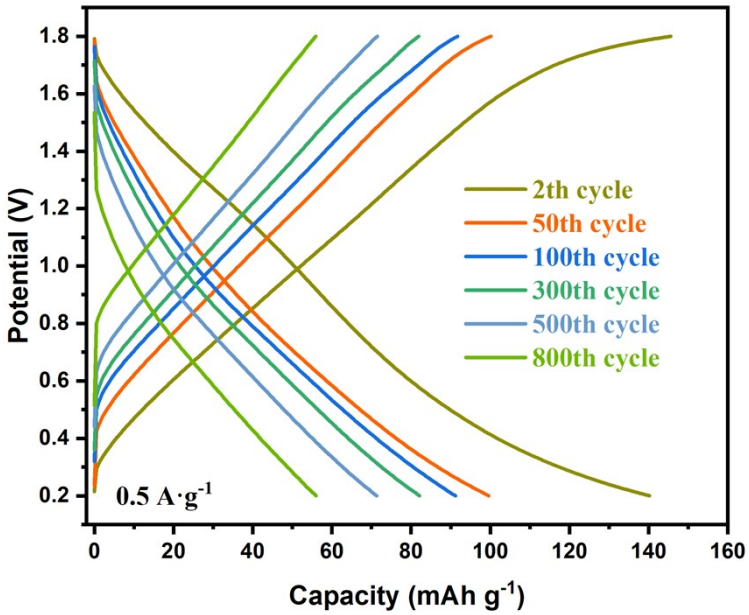

Figure S11. GCD curves of pouch cell under different cycles at 0.5 $A \cdot g^{-1}$.

Table S1. The element atomic concentration (%) of AC, AC-P5, AC-P10, and AC-P20

from XPS spectra

Sample	Contents (at%)	
	C 1s	O 1s
AC	89.14	10.86
AC-P5	88.13	11.87
AC-P10	86.28	13.72
AC-P20	88.59	11.41

Table S2. Fitted parameters for EIS plots

Sample	R_s (Ω)	R_{ct} (Ω)	R_w (Ω)
AC	2.7	71.3	0.38
AC-P5	3.2	63.8	0.41
AC-P10	3.7	59.6	0.48
AC-P20	3.3	70.8	0.44

Table S3. Comparison of the AC-P10 electrode performance with previous reports on carbon cathode materials

Concept	Capacity (mAh·g^{-1})	Ref.	Year
GPC-600	154.6 mAh·g^{-1} at 0.2 A·g^{-1}	[1]	2026
SA-3	98.9 mAh·g^{-1} at 0.1 A·g^{-1}	[2]	2024
CNPK	103.2 mAh·g^{-1} at 0.1 A·g^{-1}	[3]	2021
HPC-4	125.7 mAh·g^{-1} at 0.1 A·g^{-1}	[4]	2023
N-Macro/Meso/Micro-C	155.4 mAh·g^{-1} at 0.2 A·g^{-1}	[5]	2025
AC-P10	**171.3 mAh·g^{-1} at 0.2 A·g^{-1}**	**This work**	**2026**

References

[1] M. Liu, F. Liu, L. Hou, D. Han, L. Sheng, Z. Sun, X. Wu, X. Wang, Synthesis of nitrogen and oxygen co-doping porous carbon nanosheets for zinc-ion hybrid capacitors, Journal of Energy Storage 162 (2026) 122021.

[2] X. Pan, Q. Li, T. Wang, T. Shu, Y. Tao, Controllable synthesis of electric double-layer capacitance and pseudocapacitance coupled porous carbon cathode material for zinc-ion hybrid capacitors, Nanoscale 16(7) (2024) 3701-3713.

[3] H. Zhang, Z. Chen, Y. Zhang, Z. Ma, Y. Zhang, L. Bai, L. Sun, Boosting Zn-ion adsorption in cross-linked N/P co-incorporated porous carbon nanosheets for the zinc-ion hybrid capacitor, Journal

of Materials Chemistry A 9(30) (2021) 16565-16574.
[4] F. Mo, Y. Wang, T. Song, X. Wu, Nitrogen and oxygen co-doped hierarchical porous carbon for zinc-ion hybrid capacitor, Journal of Energy Storage 72 (2023) 108228.
[5] Y. Wu, Y. Xu, M. Tang, Y. Qiao, C. Zhang, P. Ji, O. Klimova-Korsmik, M. Kurbanov, G. Wang, Pore and doping engineering of carbon cathodes for high-performance Zn-ion capacitors, Microporous and Mesoporous Materials 395 (2025) 113703.